Title

Abrogation of fluid suppression in intracranial postcontrast fluid-attenuated inversion recovery magnetic resonance imaging: A clinical and phantom study

Journal

Veterinary Radiology & Ultrasound, 59(4)

ISSN

1058-8183

Authors

Dickinson, Peter J
Jones-Woods, Sarah
Cissell, Derek D

Publication Date

2018-07-01

DOI

10.1111/vru.12605

Peer reviewed

HHS Public Access

Author manuscript

Vet Radiol Ultrasound. Author manuscript; available in PMC 2020 September 09.

Published in final edited form as:

Vet Radiol Ultrasound. 2018 July ; 59(4): 432–443. doi:10.1111/vru.12605.

ABROGATION OF FLUID SUPPRESSION IN INTRACRANIAL POST-CONTRAST FLUID-ATTENUATED INVERSION RECOVERY MR IMAGING: A CLINICAL AND PHANTOM STUDY

PETER J. DICKINSON[1], **SARAH. JONES-WOODS**[1], **DEREK D. CISSELL**[1]

[1]Department of Surgical and Radiological Sciences, School of Veterinary Medicine, University of California, Davis.

Abstract

Post-contrast, fluid–attenuated inversion recovery (PC-T2 FLAIR) sequences are reported to be of variable value in veterinary and human neuroimaging. The source of hyperintensity in PC-T2 FLAIR images is inconsistently reported and has implications for the significance of imaging findings. We hypothesized that the main source of increased signal intensity in PC-T2 FLAIR images would be due to gadolinium leakage into adjacent fluid, and that the resulting gadolinium-induced T1 shortening causes reappearance of fluid hyperintensity, previously nulled on pre-contrast FLAIR images.

A retrospective descriptive study was carried out comparing T2 weighted (T2W), pre and post-contrasted T1 weighted (T1W) and pre and post-contrast weighted T2 FLAIR images in a variety of intracranial diseases in dogs and cats. A prospective phantom *in vitro* study was also done to compare the relative effects of gadolinium concentration on T2W, T1W and FLAIR images. A majority of hyperintensities on PC-T2 FLAIR images that were not present on pre-contrast FLAIR images were also present on pre-contrast T2W images, and were consistent with normal or pathological fluid filled structures. Phantom imaging demonstrated increased sensitivity of FLAIR sequences to low concentrations of gadolinium compared to T1W sequences.

Apparent contrast enhancement on PC-T2FLAIR images often reflects leakage of gadolinium across normal or pathology specific barriers into fluid–filled structures, and hyperintensity may therefore represent normal fluid structures as well as pathological tissues. PC-T2FLAIR images may provide insight into integrity of biological structures such as the ependymal and subarachnoid barriers that may be relevant to progression of disease.

Correspondence: Peter J. Dickinson, Department of Surgical and Radiological Sciences, School of Veterinary Medicine, University of California, Davis. pjdickinson@ucdavis.edu.

List of Author Contributions
Category 1
(a) Conception and Design: Dickinson, Cissell
(b) Acquisition of Data: Dickinson, Cissell, Jones Woods
(c) Analysis and Interpretation of Data: Dickinson, Cissell, Jones Woods
Category 2
(a) Drafting the Article: Dickinson, Cissell, Jones Woods
(b) Revising Article for Intellectual Content: Dickinson, Cissell, Jones Woods
Category 3
(a) Final Approval of the Completed Article: Dickinson, Cissell, Jones Woods

Keywords

Brain; Cat; Dog; Gadolinium; MRI

Introduction

Fluid-attenuated inversion recovery (FLAIR) sequences have been used to increase conspicuity of T2 hyperintense lesions in the vicinity of T2 hyperintense free fluid with minimal cellular or protein content, such as cerebrospinal fluid (CSF). Suppression of signal from water and normal CSF is achieved using a 180^0 radiofrequency pulse to invert the equilibrium magnetization vector (NMV) followed by a 90^0 excitation pulse applied at a specific time from inversion (TI). The TI is set to correspond to the specific moment at which normal CSF has recovered from negative longitudinal magnetization to zero longitudinal magnetization (Fig 1). As there is no longitudinal magnetization of CSF at the time of the 90^0 excitation pulse, no transverse magnetization is induced following excitation, effectively nulling signal associated with water/CSF.

Post-contrast T2 FLAIR (PC-T2FLAIR) imaging sequences have been investigated in a variety of intracranial pathologies with the goal of increasing diagnostic sensitivity. The diagnostic value of PC-T2FLAIR has been variably reported in both veterinary,[1, 2] and human studies,[3–5] with its use in meningeal based disease commonly reported as beneficial.[6–8] The mechanism for increased signal intensity on PC-T2FLAIR images is variably reported and includes mild T1 effects (in the heavily T2 weighted images), increased T1 contrast due to the use of inversion recovery (IR) sequences, magnetization transfer effects and delayed enhancement.[5] However, FLAIR imaging appears to have a high sensitivity to changes in the T1 relaxation time of CSF,[9] and contamination of CSF (or other fluids) with blood, protein or gadolinium contrast agents can alter longitudinal relaxation rates (T1) resulting in incomplete suppression of fluid signal causing hyperintensity on PC-T2FLAIR images.[3, 9–14]

We hypothesized that a large component of the signal hyperintensity seen on PC-T2FLAIR images of intracranial disease is due to gadolinium induced, local abrogation of fluid suppression and “reappearance” of hyperintensity observed on T2W images, but nulled on pre-contrast FLAIR images. Objectives of the study were: 1) to retrospectively review PC-T2FLAIR images that were acquired in selected cases where disease was closely associated with fluid filled structures such as ventricles or subarachnoid spaces and to assess PC-T2FLAIR hyperintensities and their correlation with lesions on post-contrast T1W, precontrast T2W, and precontrast T2 FLAIR images, 2) to determine the sensitivity of T1W, T2W and T2FLAIR imaging sequences to the effects of gadolinium using an *in vitro* phantom model.

Methods

Clinical patients

Clinical cases from dogs and cats undergoing MRI for intracranial disease between October 2014 and January 2017 were selected for a retrospective, descriptive study based on the presence of differences in pre and post-contrast FLAIR imaging findings. Images were acquired using a 1.5T MRI system (GE Signa, GE Healthcare, Waukesha, WI). Decisions to acquire post-contrast FLAIR images were at the discretion of the neurologist or radiologist for individual patients, and included cases where disease was closely associated with fluid filled structures such as ventricles or subarachnoid spaces. Data recorded included, species, body weight, anesthesia protocols and MRI sequences and sequence parameters. Images were reviewed by all authors using eFilmWorkstation® 3.3 (Merge Healthcare, Hartland, WI) and NEC MD21GS-3MP-CB medical diagnostic monitors (NEC Display Solutions, Itasca, Ill) and descriptive data were defined by consensus. The primary inclusion criterion was the presence of hyperintensity on post-contrast FLAIR images that was not present on pre-contrast FLAIR images. Subsequent assessment of images included determination of localization of new post-contrast FLAIR hyperintensities with reference to post-contrast T1 weighted image hyperintensity and pre-contrast T2 weighted image hyperintensity. Location of post-contrast FLAIR hyperintensity with respect to fluid filled structures as defined by T2 weighted and pre-contrast FLAIR images was also noted.

Phantom study

A prospective *in vitro* phantom study was done to assess the effect of different tissue compositions and gadolinium concentrations on MRI signal intensity. Three different materials and eleven different gadolinium concentrations were assessed in a full factorial experimental design as outlined in Table 2. Materials consisted of ultrapure, deionized water (upH_2O; Milli-Q®, EMD Millpore, Billerica, MA), upH_2O plus 2.4 g/dL bovine serum albumin (Sigma-Aldrich, St. Louis, MO), and 2% w/v agarose (Sigma-Aldrich) dissolved in upH_2O. Serial 1:1 and 1:2 dilutions dilutions of gadopentetate dimeglumine (GPDM; Magnevist, Bayer, Berlin) were prepared in each material to achieve final concentrations from 0.008 – 20.0 mM (Table 2). GPDM dilutions in agarose were prepared at ~60°C and thoroughly mixed. All spaces between and around the wells of two standard 24-well tissue culture plates were filled with blank 2% agarose solution and allowed to gel to reduce magnetic susceptibility inhomogeneity. GPDM dilutions in 2% agarose were then added to the 24-well plate and allowed to gel. Finally, aliquots of each GPDM dilution in upH_2O or upH_2O plus albumin were added to the well plates. Samples of each material without added GPDM were also added to both well plates. The two well plates were stacked and centered in a brain radiofrequency (RF) coil, and the well plates and RF coil advanced to isocenter of a 1.5T MRI system (GE Signa). T1W, T2W and T2-weighted FLAIR images of the well plates were obtained with pulse sequence details as outlined in Table 3. All images were acquired with 3.0 mm slice thickness, 15.0 cm field of view, and 320 × 224 matrix, and 0.7x phase field of view.

Images were qualitatively assessed (DDC) using image viewing software (Osirix v. 5.5.2, Pixmeo, Geneva, Switzerland), and signal intensities were measured using data analysis

software (MATLAB R2016a, MathWorks, Natick, MA) with a custom program created by one of the authors (DDC). Although qualitative and quantitative assessments were performed without *a priori* knowledge of the material concentration in each well, differences among materials and GPDM concentrations were obvious; thus, we attempted to minimize operator influence on quantitative measurements. After user-defined identification of the center of the corner wells of each well plate, the custom MATLAB program automatically created a 4 × 6 matrix of circular regions of interest (ROI's) with radius of 6 pixels (2.8 mm) for each ROI. The program calculated the spacing between wells given the corner well locations and the matrix size. The matrix of ROI's was plotted on the original DICOM image and visually assessed to ensure that each ROI contained only the material of interest in the interior of the well without including the well plate walls or the agarose between the wells. The program then calculated the mean signal intensity for each ROI. Mean signal intensity values were plotted against GPDM concentration for each material and pulse sequence without normalization or subtracting background noise.

Results

Clinical cases

Eighteen cases were reviewed and included 16 dogs with a weight range of 3.4 to 36.1kg and 2 cats with a weight range of 3.2–5.1kg. All imaging was performed under general anesthesia with supplemental oxygen in all cases and propofol continuous rate infusion in 9 dogs. Gaseous anesthesia with either isoflurane or sevoflurane was used in the remaining animals.

Images were acquired using a variety of radiofrequency/receiver coils depending on body weight and conformation. Specific imaging sequences consisted of noncontiguous 3.0mm thickness transverse slices with a 0.3mm interslice gap. Specific pulse sequence parameters are detailed in Table 1. Post-contrast images were acquired with T1 weighting followed by FLAIR imaging after administration of 0.1mmol/kg gadopentatate dimeglumine (0.5mmol/mL) (Magnevist®, Bayer HealthCare, Whippany, NJ).

Histopathological or cytological diagnosis was available for 13 cases. Specific diagnoses were: 7 cases of intracranial neoplasia (2 meningiomas, 2 glioblastomas, 1 oligodendroglioma, 2 lymphomas); 5 cases of infectious disease (3 bacterial meningitis/encephalitis, 1 feline infectious peritonitis, 1 bacterial otitis media/interna); 1 case of primary inflammatory disease (pachymeningitis). Cases with presumed diagnoses were 1 intraventricular mass (presumed choroid plexus tumor), 1 cerebello-pontine mass (presumed meningioma/histiocytic sarcoma), 2 presumed cases of meningoencephalitis of unknown origin. 1 case had no observable MRI abnormalities other than abrogation of fluid suppression secondary to a metallic susceptibility artefact.

Seventeen dogs had hyperintensity on PC-T2FLAIR that was not present on pre-contrast T2FLAIR images. One dog exhibited pre-contrast T2FLAIR hyperintensity within a lateral ventricle associated with magnetic field inhomogeneity due to a metal spring in the endotracheal tube cuff (Fig 8). In this dog, the hyperintensity was absent from repeat T2FLAIR images following removal of the spring. In all 18 dogs, the hyperintensity

observed on T2FLAIR / PC-T2FLAIR images also appeared hyperintense on pre-contrast T2W images.

Contrast enhancement was observed associated with the choroid plexus in 16 of 17 dogs for which T2FLAIR images were obtained after IV gadolinium contrast administration. PC-T2FLAIR enhancement was observed associated with the choroid plexus in the lateral ventricles (14 dogs), fourth ventricle (13 dogs), and/or third ventricle (3 dogs). In one dog, the choroid plexus was completely obscured by extensive intraventricular pathology. PC-T2FLAIR hyperintensity was observed in the ventricular system of 13 dogs; in all 13 dogs, fluid signal in the ventricles nulled on pre-contrast T2FLAIR images. Ventricular contrast enhancement was observed in the lateral ventricles (5 dogs), third ventricle (3 dogs), and/or fourth ventricle (6 dogs). Two dogs exhibited hyperintensity in the mesencephalic aqueduct and 2 dogs exhibited contrast enhancement of the pineal recess of the third ventricle without other ventricular hyperintensity on PC-T2FLAIR images.

Hyperintensity involving the subarachnoid space/meninges was observed on PC-T2FLAIR that was not present on pre-contrast T2FLAIR images in 13 dogs; hyperintensity was present around the cerebrum (7 dogs), cerebellum (2 dogs), midbrain or brainstem (8 dogs), and/or around the cervical spinal cord (5 dogs). PC-T2FLAIR hyperintensity was associated with “cystic” appearing accumulations of fluid in 5 dogs (Fig 5). Four dogs had intratumoral fluid accumulations and one dog had a parenchymal fluid accumulation that nulled on pre-contrast T2FLAIR and appeared hyperintense on PC-T2FLAIR. PC-T2FLAIR hyperintensity was also observed within non fluid portions of masses (defined by absence of suppression on T2FLAIR sequences) (3 dogs), brain parenchyma (1 dog), and the cochlea and tympanic bulla (1 dog).

Fifteen of 17 dogs had new or different patterns of contrast enhancement on PC-T2FLAIR images compared to post-contrast T1W images. New regions of contrast enhancement were associated with the ventricles in 9 dogs, with the subarachnoid space/meninges in 5 dogs, and with tumor or parenchymal fluid pockets in 4 dogs. Two dogs had a leptomeningeal pattern of contrast enhancement on PCT2-FLAIR images (following the anatomy of the sulci), with a pachymeningeal pattern of contrast enhancement on post-contrast T1W images. Contrast enhancement at the same location was noted to be more conspicuous on PCT2-FLAIR images compared to T1W images in the subarachnoid space/meninges, the solid portion of a mass, and the cochlea plus tympanic bulla of one dog each.

Phantom Data Results

The effect of GPDM concentration ([GPDM]) on qualitative appearance of upH_2O, upH_2O plus 2.4 g/dL albumin, and 2% agarose are depicted in Figure 2 and signal intensity measurements for water and agarose are presented in Figure 3. In the absence of GPDM, all three materials appeared hypointense on T1W and FLAIR images. Increasing [GPDM] induced increased signal intensity on T1W and FLAIR images, with peak signal intensity occurring at 2.22 mM on T1W images and at 0.278 mM for FLAIR images. upH_2O, upH_2O plus 2.4 g/dL albumin, and 2% agarose all remained hyperintense relative to baseline on T1W images for [GPDM] up to 20.0 mM. Signal intensity decreased below baseline on FLAIR images for [GPDM] greater than 2.22 mM. On T2W images, signal intensity

increased slightly up to [GPDM] of 0.278 mM, but decreased below baseline with further added GPDM. The peak signal intensity of upH_2O plus albumin was slightly lower than upH_2O on FLAIR and T1W images, but their signal intensities were nearly identical for GPDM ≤ 0.139mM (FLAIR) and GPDM ≤ 1.11mM (T1W).

Discussion

The reported cases and phantom data presented demonstrate increased sensitivity of T2 weighted FLAIR imaging to the paramagnetic effects of gadolinium in the context of free fluid. “New” lesions (not present on pre-contrast FLAIR or post-contrast T1W images) on PC-T2FLAIR images primarily result from abrogation of fluid signal suppression due to gadolinium leakage into fluid filled structures that initially appear hypointense on pre-contrast T2FLAIR images, rather than additional pathological lesions. As such, PC-T2FLAIR hyperintensities involving anatomical fluid filled structures may have biological implications for the integrity of physiological barriers within the central nervous system.

Although gadolinium induced shortening of tissues’ T1 relaxation times underlies the hyperintensity observed on both standard T1W and T2FLAIR images, the mechanism differs between the two different pulse sequences. On T1W images, shortening of T1 relaxation times in the presence of GPDM increases signal intensity due to increased longitudinal recovery. In the case of T2FLAIR images, shortening the T1 relaxation time of CSF via addition of GPDM results in longitudinal magnetization greater than zero at the specific T2FLAIR sequence inversion time resulting in abrogation of fluid signal suppression and “reappearance” of fluid hyperintensity. (Figs 1–3). Differences in T1 relaxation times have the potential to alter tissue signal intensities, even on heavily T2 weighted FLAIR images[15–19] such as T2FLAIR. This behavior was observed on *in vitro* T2W images in the current study (Figs 2, 3) but is generally not easily discernable qualitatively in the clinical setting on T2W images.[17–20]

In addition to shortening T1 relaxation time, gadolinium also shortens T2 relaxation times. This effect results in decreasing signal intensity that dominates image characteristics only at high concentrations of GPDM,[5, 20] as seen in the *in vitro* study (Figs 2,3). In the clinical setting “masking” of signal due to T2 shortening effects is not likely with standard gadolinium doses.[18] A standard 0.1mmol/kg GDPM dose would result in a plasma concentration of <2.22mM and a tissue concentration likely well below this. At these levels *in vitro*, there was no decrease in T1 signal intensity, and intensity on FLAIR imaging *in vitro* was still increased compared to baseline (Figs 2,3).

The localization of PC-T2FLAIR hyperintensities in fluid filled structures in the current case series agrees with the abrogation of fluid suppression mechanism and with similar previously reported data (Figs 4–7).[3, 9–14] Previous veterinary studies, and many human studies do not provide correlative T2W imaging data, although Kubota *et al*[21] correlated level of T2 signal with PC-T2FLAIR lesions, and similar to our findings, Merhof et al[1] noted that “new” lesions were visible on T2W images. The discrepancy between pre and post-contrast FLAIR images noted in one veterinary study[1] are also compatible with the reappearance of previously nulled fluid signal.

Consistent with the increased sensitivity to the presence of low concentrations of gadolinium with T2FLAIR compared to T1weighted sequences (Figs 2,3)[4, 5, 9, 13] we did not see enhancement of CSF on T1W post-contrast images in cases where PC-T2FLAIR findings were present, and when CSF could be clearly defined as separate from the primary pathology (e.g. in ventricles distant from T1C enhancing primary disease).(Fig 4) Gadolinium has been documented in the CSF of normal and pathological dog brains and in humans following standard doses (~0.1mmol/kg),[9, 22, 23] and contrast enhancement of subarachnoid, ventricular and cystic fluids on T1W images has been sporadically reported.[23–28] The concentration of gadolinium observed in the CSF of a normal dog (0.007 mM) following standard dosage[9] is below the concentration of gadolinium causing increased signal intensity on either T1W or T2FLAIR images in our *in vitro* study, and enhancement of CSF on T1W imaging is generally only seen with extended time delays (beyond standard imaging times) or with elevated gadolinium dosage.[9, 22]

Many studies report a benefit from PC-T2FLAIR imaging with superficial or meningeal based disease, or disease close to fluid filled structures,[3, 5, 29–31] likely due to abrogation of fluid suppression in the subarachnoid space or other fluids as has been shown specifically for ischemic injury.[12, 13] Limited resolution of meningeal vs subarachnoid location of signal precludes this conclusion definitively in all cases in the current study (e.g. Figs 6, 7), although more easily defined location of signal in the ventricular CSF provides strong evidence for this mechanism. This is particularly true when PC-T2FLAIR “lesions” extend down the ventricular system away from the primary lesion location (Fig 4).

Hyperintensity of choroid plexus was a consistent finding on PC-T2FLAIR in this study and has been reported previously in humans.[4, 32] Location of choroid plexus within the fluid space of the ventricles makes assessment of its “fluid-associated/T2 hyperintense” MR characteristics difficult. Normal leakage of gadolinium across the choroid plexus endothelium into the high fluid content plasma ultrafiltrate within the stroma could provide a mechanism for the PC-T2FLAIR hyperintensity observed.

Leakage of gadolinium into fluid compartments via compromised anatomical and physiological barriers within the CNS, has implications for pathobiology in a variety of disease conditions, in addition to simple definition of neuroanatomical localization. Post-gadolinium CSF “enhancement” on FLAIR imaging has been proposed as an early, sensitive predictor of blood-brain barrier disruption in ischemic injury,[12, 13, 33] and has been termed the “Hyperintense Acute Reperfusion Marker” (HARM). The hyperintensity has been shown to be the result of gadolinium leakage into the CSF rather than parenchymal enhancement,[12, 13] and has potential implications for prognosis. PC-T2FLAIR defined involvement of multiple ventricular compartments demonstrated for both infectious/inflammatory disease and particularly with neoplastic disease in the current study suggests the potential for disease extension beyond compromised physiological barriers. Similarly, iatrogenic compromise of meningeal barriers secondary to intracranial surgical procedures has potential implications for local disease extension. Post-surgical contrast enhancement of meninges on T1W images is a common finding in humans and dogs,[34] and PC-T2FLAIR signal associated with this transient T1W post-contrast enhancement of meninges was seen in this series (Fig 7) and has also been reported previously.[3] Nulling of endoperilymphatic fluid of the inner ear is

seen on FLAIR imaging similar to that of CSF, and PC-T2FLAIR imaging has been shown to have increased sensitivity to breakdown of the blood-labyrinthine barrier compared to T1W post-contrast imaging.[35–37] The positive PC-T2FLAIR findings unilaterally, (consistent with clinical signs) was informative in the case of otitis media/interna when disease was present in both middle ear cavities (Fig 6).

Several confounding factors were present in the current study. Assessing sensitivity of PC-T2FLAIR images compared to other sequences was not the goal of this study, and bias in case selection was large. Sequence acquisition order was not randomized, and all PC-T2FLAIR images were acquired after post-contrast T1W images. Delayed enhancement is well documented on standard T1W sequences[9, 22, 23, 38–40] and also potentially on sequences with long TR[5, 18] however this would be unlikely to alter conclusions relating to spatial location of PC-T2FLAIR hyperintensities. Anesthesia related hyperintensity of CSF on FLAIR imaging has also been reported associated with supplemental oxygen and propofol, [41, 42] which were used in a majority of the current cases, however effects should have been present on both pre and post-contrast FLAIR images. Similarly, ghosting artefacts from CSF flow would also be expected to be present in pre and post-contrast images. We did recognize an artefactual increase in CSF signal on precontrat FLAIR images in one case (Fig 8) where local magnetic field inhomogeneity associated with a metal endotracheal cuff spring resulted in spatially-varying incomplete inversion of longitudinal magnetization and abrogation of fluid signal suppression.[43] In this case CSF hyperintensity was not present in post-contrast FLAIR images once the ferromagnetic material was removed.

The data presented are supportive of a mechanism for PC-T2FLAIR hyperintensity based on abrogation of fluid nulling following leakage of gadolinium into accumulations of free fluid adjacent to primary disease. This is consistent with the majority of reports where benefits of PC-T2FLAIR imaging are seen in meningeal, superficial, or fluid associated lesions and where “new” lesions are correlated with precontrast T2 hyperintensity. We suggest that the value of PC-T2FLAIR imaging should not be judged solely on the basis of sensitivity to “additional lesions”, since presence of PC-T2FLAIR signal may have additional implications to T1W post-contrast signal in the same general location with respect to integrity of physiological barriers. Future studies may investigate whether breakdown of ependymal barriers, implicated by PC-T2FLAIR ventricular CSF signal, is correlated with a higher incidence of intraventricular metastasis for tumors adjacent to ventricular structures, or whether increased sensitivity of inversion sequences may improve delineation of subtle disease involving vestibular/cochlear structures or intradural segments of cranial and peripheral nerve roots.

Acknowledgements

The authors thank Rich Larson, Jason Peters and Jennifer Larsen for assistance with MR image acquisition, and Dr Gregg Kortz for case contribution.

References

1. Merhof K, Lang J, Durr S, Stahl C, Gorgas D. Use of contrast-enhanced fluid-attenuated inversion recovery sequence to detect brain lesions in dogs and cats. J Vet Intern Med. 2014;28: 1263–1267. [PubMed: 24962604]
2. Falzone C, Rossi F, Calistri M, Tranquillo M, Baroni M. Contrast-enhanced fluid-attenuated inversion recovery vs. contrast-enhanced spin echo T1-weighted brain imaging. Vet Radiol Ultrasound. 2008;49: 333–338. [PubMed: 18720762]
3. Bozzao A, Floris R, Fasoli F, Fantozzi LM, Colonnese C, Simonetti G. Cerebrospinal fluid changes after intravenous injection of gadolinium chelate: assessment by FLAIR MR imaging. Eur Radiol. 2003;13: 592–597. [PubMed: 12594563]
4. Lee EK, Lee EJ, Kim S, Lee YS. Importance of Contrast-Enhanced Fluid-Attenuated Inversion Recovery Magnetic Resonance Imaging in Various Intracranial Pathologic Conditions. Korean J Radiol. 2016;17: 127–141. [PubMed: 26798225]
5. Mathews VP, Caldemeyer KS, Lowe MJ, Greenspan SL, Weber DM, Ulmer JL. Brain: gadolinium-enhanced fast fluid-attenuated inversion-recovery MR imaging. Radiology. 1999;211: 257–263. [PubMed: 10189481]
6. Tsuchiya K, Katase S, Yoshino A, Hachiya J. FLAIR MR imaging for diagnosing intracranial meningeal carcinomatosis. AJR Am J Roentgenol. 2001;176: 1585–1588. [PubMed: 11373237]
7. Absinta M, Vuolo L, Rao A, Nair G, Sati P, Cortese IC, et al. Gadolinium-based MRI characterization of leptomeningeal inflammation in multiple sclerosis. Neurology. 2015;85: 18–28. [PubMed: 25888557]
8. Splendiani A, Puglielli E, De Amicis R, Necozione S, Masciocchi C, Gallucci M. Contrast-enhanced FLAIR in the early diagnosis of infectious meningitis. Neuroradiology. 2005;47: 591–598. [PubMed: 16034600]
9. Mamourian AC, Hoopes PJ, Lewis LD. Visualization of intravenously administered contrast material in the CSF on fluid-attenuated inversion-recovery MR images: an in vitro and animal-model investigation. AJNR Am J Neuroradiol. 2000;21: 105–111. [PubMed: 10669233]
10. Essig M, Bock M. Contrast optimization of fluid-attenuated inversion-recovery (FLAIR) MR imaging in patients with high CSF blood or protein content. Magn Reson Med. 2000;43: 764–767. [PubMed: 10800044]
11. Jagannathan J, Walbridge S, Butman JA, Oldfield EH, Lonser RR. Effect of ependymal and pial surfaces on convection-enhanced delivery. J Neurosurg. 2008;109: 547–552. [PubMed: 18759589]
12. Henning EC, Latour LL, Warach S. Verification of enhancement of the CSF space, not parenchyma, in acute stroke patients with early blood-brain barrier disruption. J Cereb Blood Flow Metab. 2008;28: 882–886. [PubMed: 18091756]
13. Kohrmann M, Struffert T, Frenzel T, Schwab S, Doerfler A. The hyperintense acute reperfusion marker on fluid-attenuated inversion recovery magnetic resonance imaging is caused by gadolinium in the cerebrospinal fluid. Stroke. 2012;43: 259–261. [PubMed: 21980209]
14. Naganawa S The Technical and Clinical Features of 3D-FLAIR in Neuroimaging. Magn Reson Med Sci. 2015;14: 93–106. [PubMed: 25833275]
15. Hendrick RE, Raff U. Image contrast and noise In: Stark DD, Bradley WD (eds): Magnetic Resonance Imaging. St Louis, MO: Mosby-Yearbook, 1992;123–129.
16. Hesselink JR, Healy ME, Press GA, Brahme FJ. Benefits of Gd-DTPA for MR imaging of intracranial abnormalities. J Comput Assist Tomogr. 1988;12: 266–274. [PubMed: 3351041]
17. Mihara F, Gupta KL, Righi AM. Non-T1-weighted spin-echo MR imaging with contrast material: experimental and preliminary clinical assessment. Radiation medicine. 1994;12: 209–212. [PubMed: 7863024]
18. Wessbecher FW, Maravilla KR, Dalley RW. Optimizing brain MR imaging protocols with gadopentetate dimeglumine: enhancement of intracranial lesions on spin-density- and T2-weighted images. AJNR Am J Neuroradiol. 1991;12: 675–679. [PubMed: 1882743]
19. Hendrick RE, Haacke EM. Basic physics of MR contrast agents and maximization of image contrast. Journal of magnetic resonance imaging : JMRI. 1993;3: 137–148. [PubMed: 8428081]

20. Runge VM, Clanton JA, Herzer WA, Gibbs SJ, Price AC, Partain CL, et al. Intravascular contrast agents suitable for magnetic resonance imaging. Radiology. 1984;153: 171–176. [PubMed: 6433402]
21. Kubota T, Yamada K, Kizu O, Hirota T, Ito H, Ishihara K, et al. Relationship between contrast enhancement on fluid-attenuated inversion recovery MR sequences and signal intensity on T2-weighted MR images: visual evaluation of brain tumors. Journal of magnetic resonance imaging : JMRI. 2005;21: 694–700. [PubMed: 15906343]
22. Knutzon RK, Poirier VC, Gerscovich EO, Brock JM, Buonocore M. The effect of intravenous gadolinium on the magnetic resonance appearance of cerebrospinal fluid. Invest Radiol. 1991;26: 671–673. [PubMed: 1885275]
23. Naul LG, Finkenstaedt M. Extensive cerebrospinal fluid enhancement with gadopentetate dimeglumine in a primitive neuroectodermal tumor. AJNR Am J Neuroradiol. 1997;18: 1709–1711. [PubMed: 9367319]
24. Pui MH, Langston JW, Arai Y. Gd-DTPA enhancement of CSF in meningeal carcinomatosis. J Comput Assist Tomogr. 1993;17: 940–944. [PubMed: 8227581]
25. Sakamoto S, Kitagaki H, Ishii K, Yamaji S, Ikejiri Y, Mori E. Gadolinium enhancement of the cerebrospinal fluid in a patient with meningeal fibrosis and cryptococcal infection. Neuroradiology. 1997;39: 504–505. [PubMed: 9258928]
26. Berger B, Ortiz O, Gold A, Hilal SK. Total cerebrospinal fluid enhancement following intravenous Gd-DTPA administration in a case of meningiomatosis. AJNR Am J Neuroradiol. 1992;13: 15–18. [PubMed: 1595433]
27. Good CD, Jager HR. Contrast enhancement of the cerebrospinal fluid on MRI in two cases of spirochaetal meningitis. Neuroradiology. 2000;42: 448–450. [PubMed: 10929307]
28. Suzuki M, Takashima T, Kadoya M, Konishi H, Kawamori Y, Ueda F, et al. Contrast enhancement of cystic portions in brain tumors on delayed image of gadolinium-DTPA-enhanced MR imaging. Radiation medicine. 1991;9: 14–18. [PubMed: 1852900]
29. Zhou ZR, Shen TZ, Chen XR, Peng WJ. Diagnostic value of contrast-enhanced fluid-attenuated inversion-recovery MRI for intracranial tumors in comparison with post-contrast T1W spin-echo MRI. Chin Med J (Engl). 2006;119: 467–473. [PubMed: 16584644]
30. Ercan N, Gultekin S, Celik H, Tali TE, Oner YA, Erbas G. Diagnostic value of contrast-enhanced fluid-attenuated inversion recovery MR imaging of intracranial metastases. AJNR Am J Neuroradiol. 2004;25: 761–765. [PubMed: 15140715]
31. Vaswani AK, Nizamani WM, Ali M, Aneel G, Shahani BK, Hussain S. Diagnostic Accuracy of Contrast-Enhanced FLAIR Magnetic Resonance Imaging in Diagnosis of Meningitis Correlated with CSF Analysis. ISRN Radiol. 2014;2014: 578986. [PubMed: 24977138]
32. Goo HW, Choi CG. Post-contrast FLAIR MR imaging of the brain in children: normal and abnormal intracranial enhancement. Pediatr Radiol. 2003;33: 843–849. [PubMed: 14551756]
33. Kang K, Lee S. Hyperintensity in the subarachnoid space on contrast-enhanced fluid-attenuated inversion-recovery magnetic resonance imaging after central venous catheter removal. J Thromb Thrombolysis. 2013;36: 346–347. [PubMed: 23733105]
34. Chow KE, Tyrrell D, Long SN. Early Postoperative Magnetic Resonance Imaging Findings in Five Dogs with Confirmed and Suspected Brain Tumors. Vet Radiol Ultrasound. 2015;56: 531–539. [PubMed: 26372362]
35. Sone M, Mizuno T, Naganawa S, Nakashima T. Imaging analysis in cases with inflammation-induced sensorineural hearing loss. Acta Otolaryngol. 2009;129: 239–243. [PubMed: 18720058]
36. Sugiura M, Naganawa S, Teranishi M, Nakashima T. Three-dimensional fluid-attenuated inversion recovery magnetic resonance imaging findings in patients with sudden sensorineural hearing loss. Laryngoscope. 2006;116: 1451–1454. [PubMed: 16885752]
37. Berrettini S, Seccia V, Fortunato S, Forli F, Bruschini L, Piaggi P, et al. Analysis of the 3-dimensional fluid-attenuated inversion-recovery (3D-FLAIR) sequence in idiopathic sudden sensorineural hearing loss. JAMA Otolaryngol Head Neck Surg. 2013;139: 456–464. [PubMed: 23681028]

38. Kushnirsky M, Nguyen V, Katz JS, Steinklein J, Rosen L, Warshall C, et al. Time-delayed contrast-enhanced MRI improves detection of brain metastases and apparent treatment volumes. J Neurosurg. 2016;124: 489–495. [PubMed: 26361281]

39. Schorner W, Laniado M, Niendorf HP, Schubert C, Felix R. Time-dependent changes in image contrast in brain tumors after gadolinium-DTPA. AJNR Am J Neuroradiol. 1986;7: 1013–1020. [PubMed: 3098065]

40. Yuh WT, Tali ET, Nguyen HD, Simonson TM, Mayr NA, Fisher DJ. The effect of contrast dose, imaging time, and lesion size in the MR detection of intracerebral metastasis. AJNR Am J Neuroradiol. 1995;16: 373–380. [PubMed: 7726087]

41. Deliganis AV, Fisher DJ, Lam AM, Maravilla KR. Cerebrospinal fluid signal intensity increase on FLAIR MR images in patients under general anesthesia: the role of supplemental O2. Radiology. 2001;218: 152–156. [PubMed: 11152794]

42. Filippi CG, Ulug AM, Lin D, Heier LA, Zimmerman RD. Hyperintense signal abnormality in subarachnoid spaces and basal cisterns on MR images of children anesthetized with propofol: new fluid-attenuated inversion recovery finding. AJNR Am J Neuroradiol. 2001;22: 394–399. [PubMed: 11156789]

43. Stuckey SL, Goh TD, Heffernan T, Rowan D. Hyperintensity in the subarachnoid space on FLAIR MRI. AJR Am J Roentgenol. 2007;189: 913–921. [PubMed: 17885065]

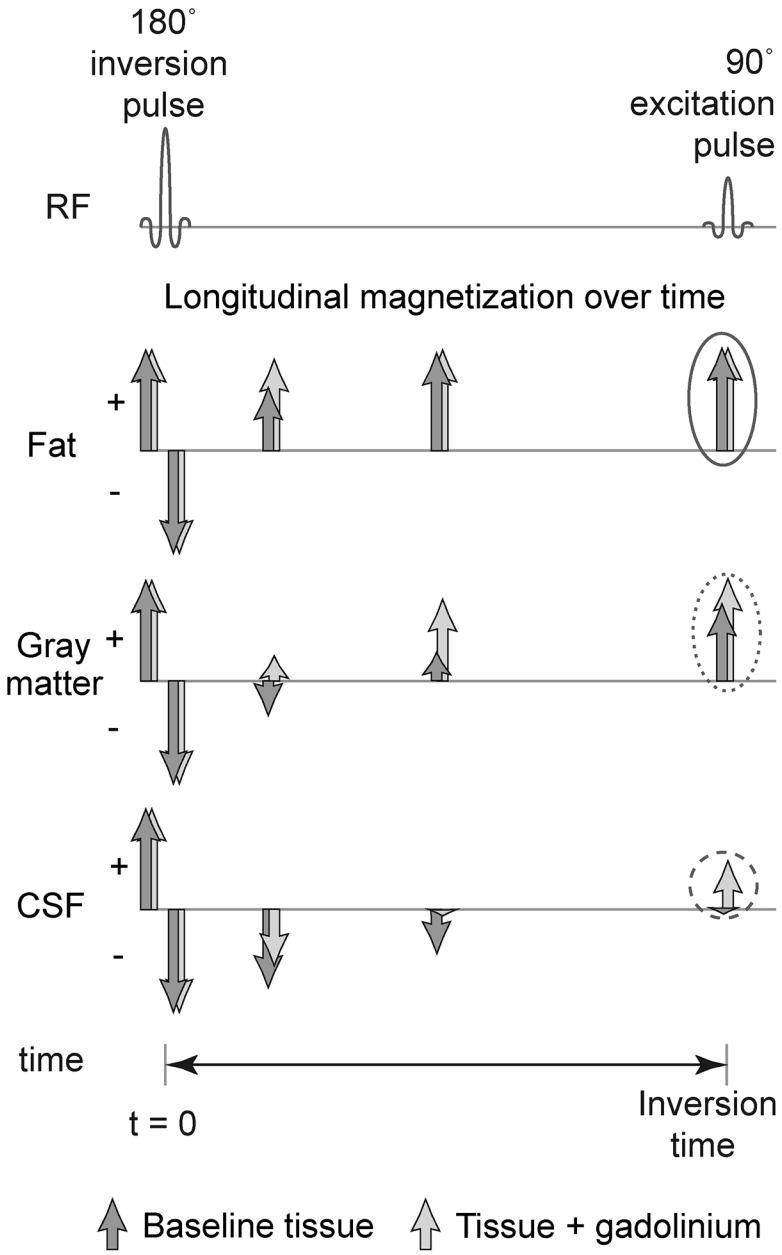

Fig 1.

Evolution of longitudinal magnetization (M_Z) for different tissues without (dark gray arrows) and with added gadolinium (light gray arrows) between the inversion pulse and excitation pulse of a typical fluid attenuating inversion recovery pulse sequence. The magnitude of M_Z at the time of excitation determines the maximum possible signal intensity of a tissue in the resulting image. A 180° inversion pulse flips the equilibrium M_Z from positive to negative, and then M_Z recovers for each tissue according to their T1 relaxation times. Short to intermediate T1 relaxation times result in negligible gain in M_Z for fat (solid oval) and a small gain of M_Z for brain gray matter (dotted oval). In the absence of gadolinium, M_Z of normal cerebrospinal fluid (CSF) reaches the null point at the inversion time and contributes zero signal to the image. Addition of gadolinium to CSF causes M_Z to

cross the null point prior to the inversion time, resulting in positive M_Z that contributes signal to the image (dashed circles). RF = radiofrequency.

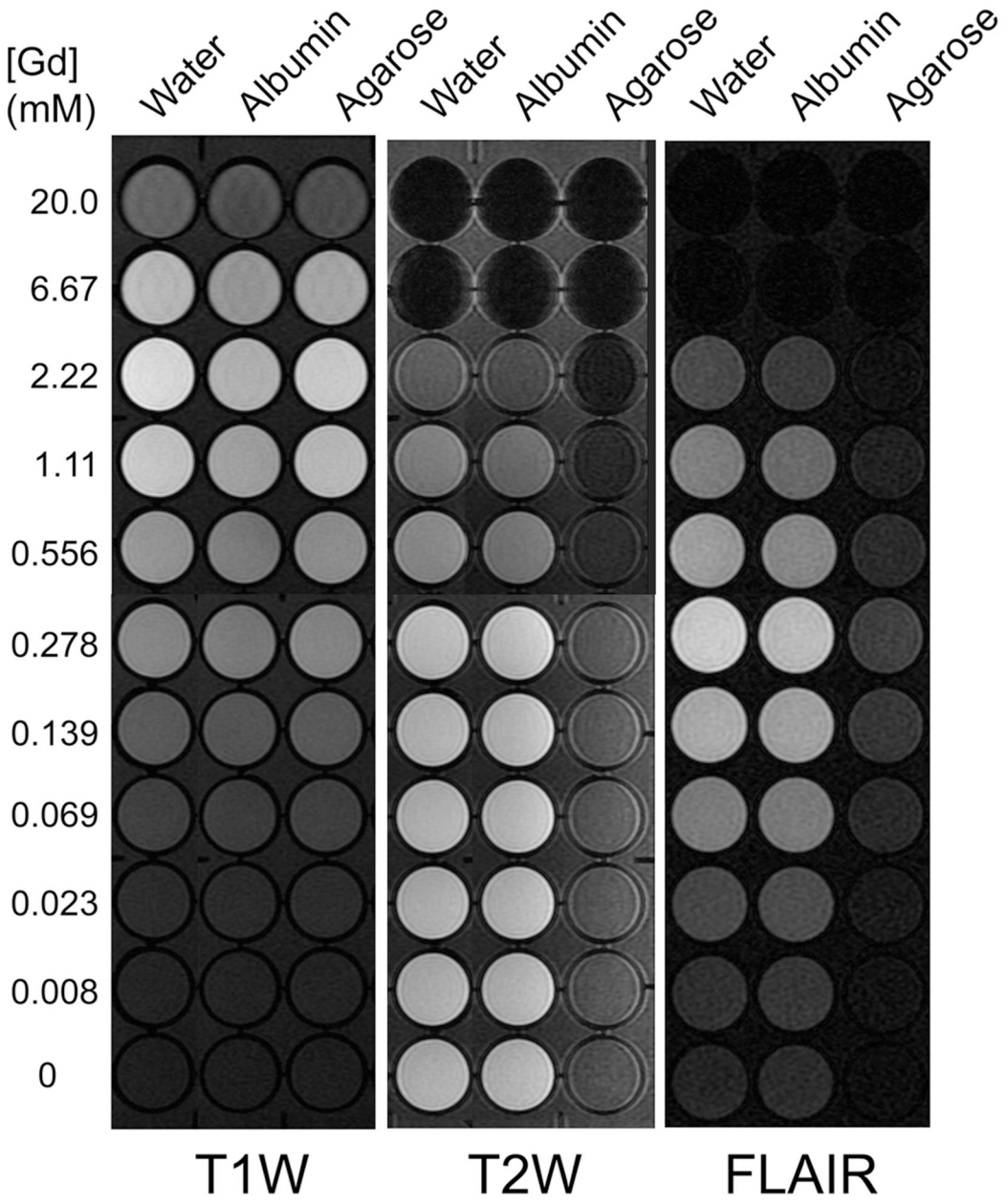

Fig 2.

Effect of gadopentetate dimeglumine (GPDM) concentration on the qualitative appearance of water (Water), water + 2.4 g/dL bovine serum albumin (Albumin), and 2% w/v agarose (Agarose) on T1-weighted (T1W), T2-weighted (T2W), and T2-weighted fluid attenuating inversion recovery (PC-T2FLAIR) images. Conspicuous contrast enhancement of water is observed at lower gadolinium concentrations on FLAIR images than on T1W images, but signal intensity decreases on T2W and FLAIR images at concentration of gadolinium (>0.28 mM). All images are displayed with window width = 2000 and window level = 1000.

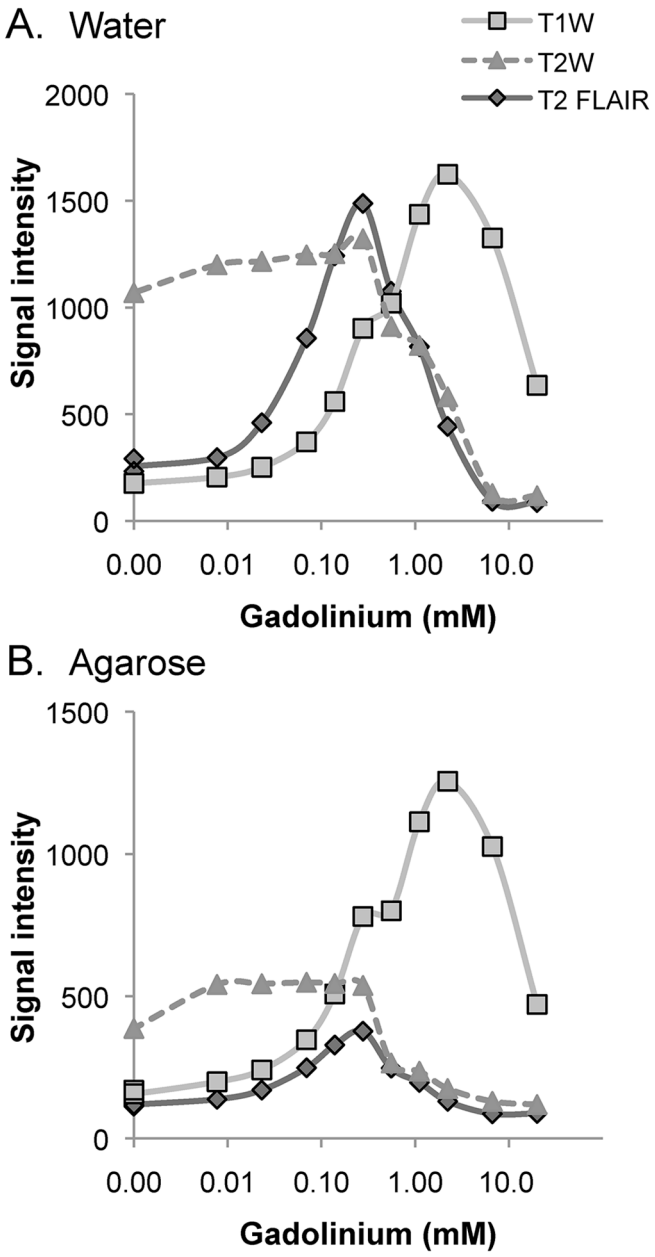

Fig 3.

Signal intensity of water (A) and 2% agarose (B) as a function of gadopentetate dimeglumine (GPDM) concentration for T1-weighted (T1W), T2-weighted (T2W), and T2-weighted fluid attenuating inversion recovery (FLAIR) images. Signal intensity of water peaks at lower concentrations of GPDM on FLAIR images than on T1W images. Agarose exhibits a modest (3.3x) peak increase in signal intensity on FLAIR images compared to the marked (7.4x) increase in signal intensity apparent on T1W images.

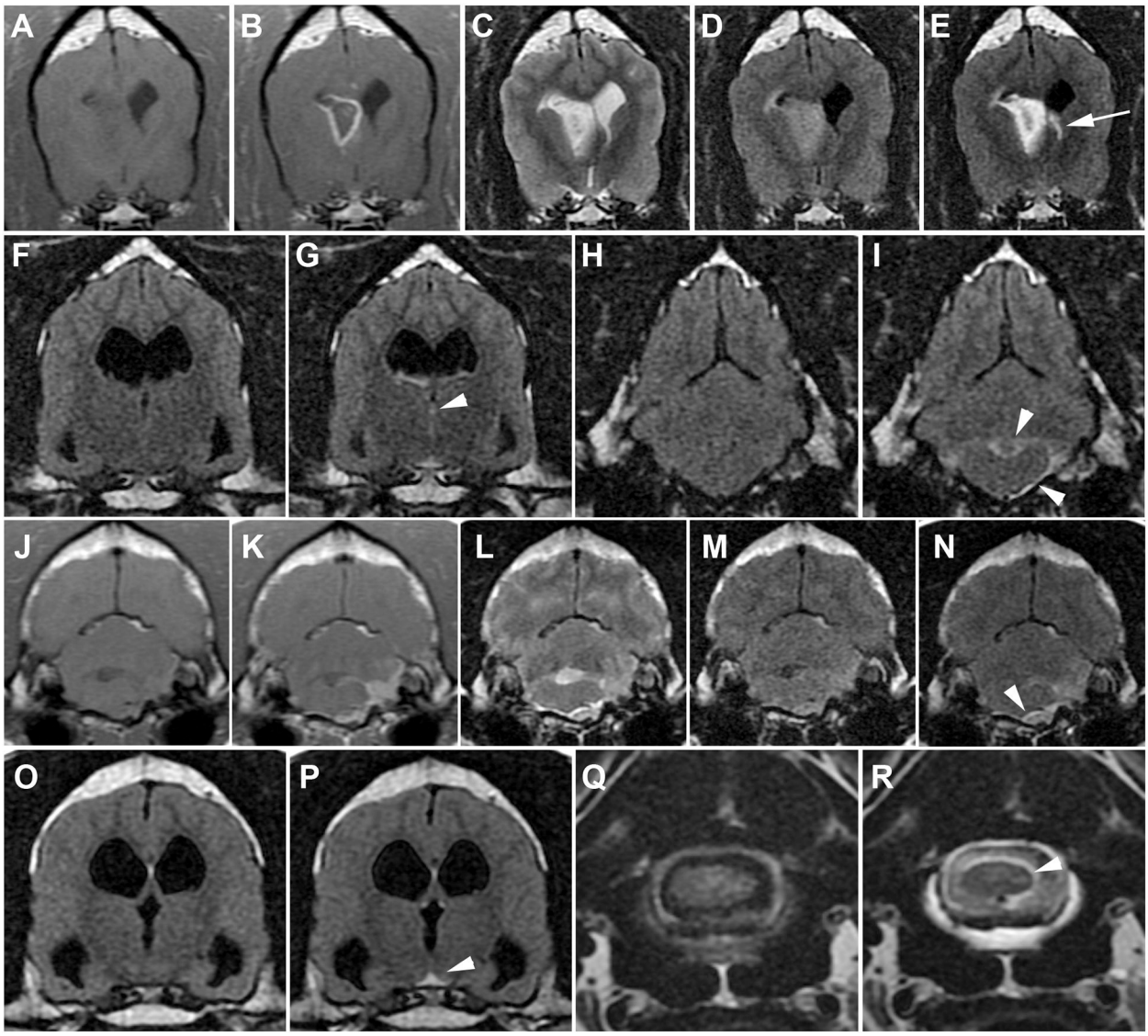

Fig 4.

PC-T2FLAIR hyperintensity involving ventricular structures distant to primary lesions. A-E and J-N (T1W, T1W + contrast, T2W, FLAIR and FLAIR + contrast images) (F, H, O, Q pre-contrast FLAIR, G, I, P, R post-contrast FLAIR). PC-T2FLAIR hyperintensity (E, arrow) is present involving the lateral ventricle contralateral to an oligodendroglioma impinging on the opposite ventricle. Hyperintensity is also seen involving the 3rd ventricle (G), 4th ventricle and adjacent subarachnoid space (H) distal to the tumor (arrowheads). PC-T2FLAIR hyperintensity associated with an extraaxial caudal fossa mass (N, arrowhead) is also present involving the 3rd ventricle (P, arrowhead) and C1 spinal cord subarachnoid space (R, arrowhead), also distant from the primary lesion. PC-T2FLAIR hyperintensities localize spatially with T2 hyperintensities that are suppressed on pre-contrast FLAIR imaging.

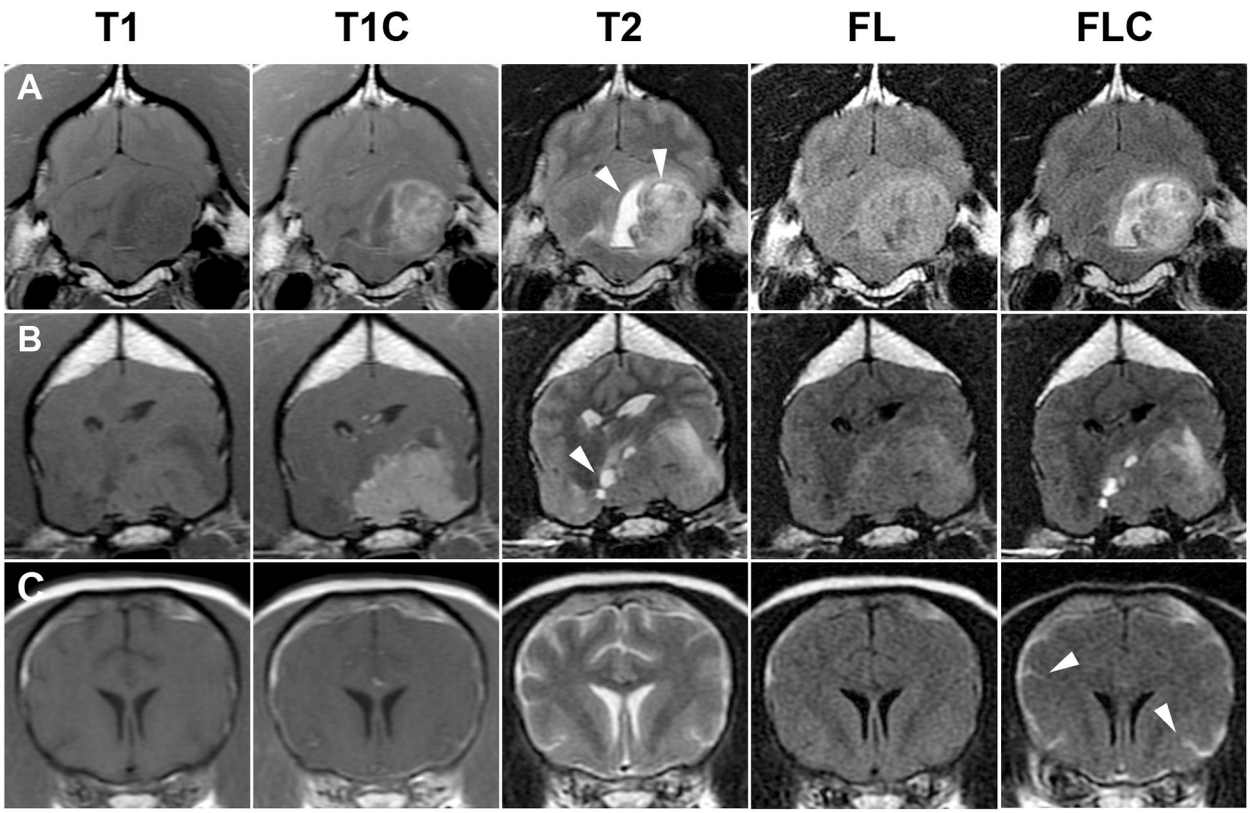

Fig 5.

Caudal fossa glioblastoma (A), meningioma (B) and lymphoma (C). Hyperintensity associated with intratumoral fluid accumulations present on T2W images (arrowheads, A, B) is suppressed on FLAIR images and reappears on PC-T2FLAIR images due to loss of fluid signal suppression. Leptomeningeal infiltration by lymphoma (C) with associated delineation of sulcal subarachnoid CSF on PC-T2FLAIR images (C, arrowheads) is more extensive than on T1W post-contrast images.

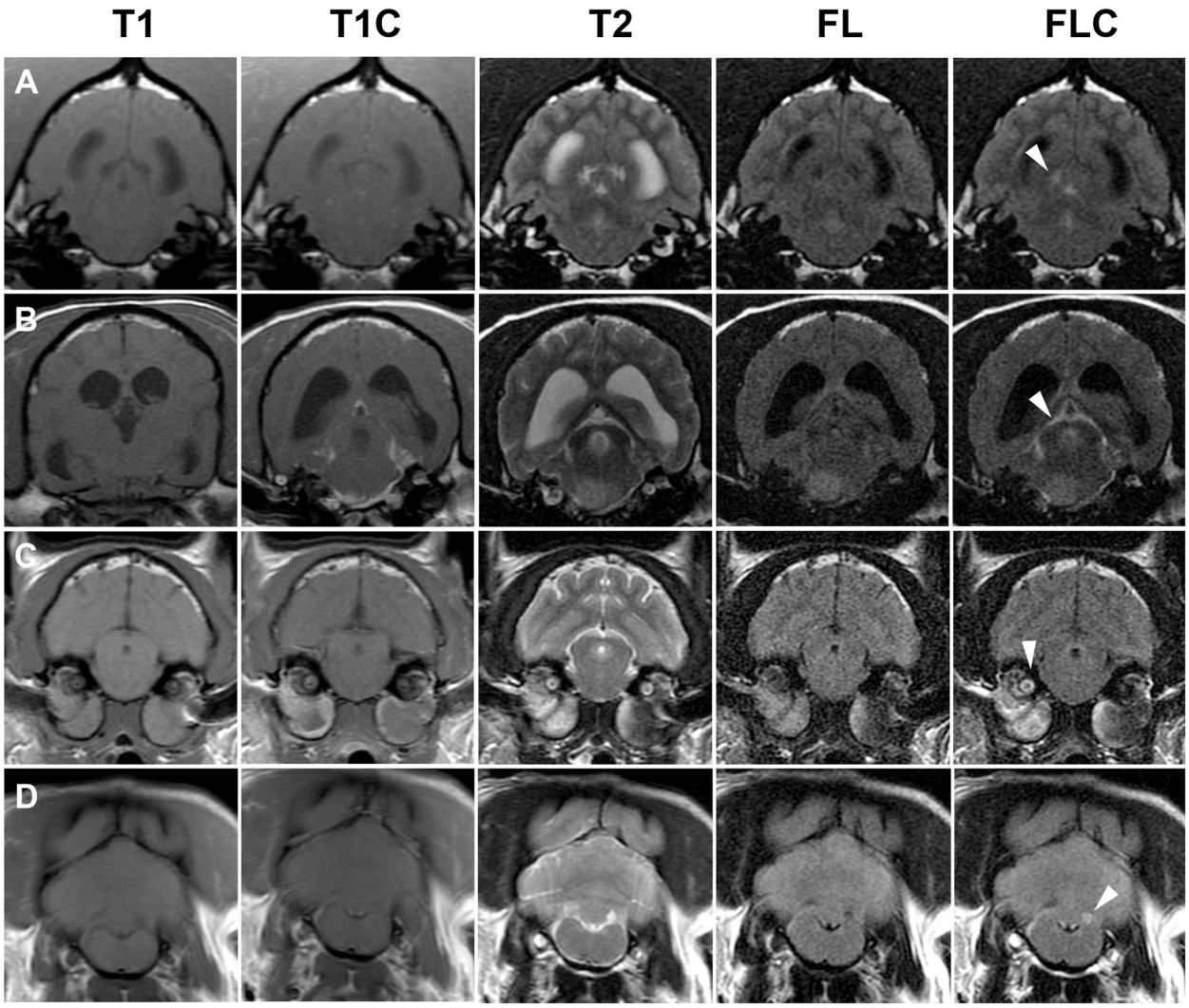

Fig 6.

Bacterial meningoencephalitis (A, B), bacterial otitis media-interna (C) and meningoencephalitis of undetermined origin (presumed immune–mediated) (D). PC-T2FLAIR hyperintensities (arrowheads) not associated with T1W post-contrast signal can be seen associated with both ventricular (A) and subarachnoid (B) structures, and correlating with T2W hyperintensities that are suppressed on FLAIR images. Abrogation of labyrinthine fluid suppression in the cochlea on the right side (C, arrowhead) correlated with clinical signs of vestibular dysfunction in a cat with bilateral disease. Asymmetrical enhancement of the cochlea on T1C images is present though less conspicuous. Loss of fluid suppression on PC-T2FLAIR images with no associated post-contrast T1W signal (D, arrowhead) is present in a dog with inflammatory CSF, and correlates with T2W hyperintensity.

Fig 7.

Post-operative, PC-T2FLAIR hyperintensity associated with the local subarachnoid spaces following removal of an olfactory/frontal lobe meningioma. Pre-surgery transverse T1W post-contrast image (A), post-surgery T1W (B), T1W post-contrast (C), T2W (D), FLAIR (E) and PC-T2FLAIR (F) images. While post-surgery T1W post-contrast and PC-T2FLAIR hyperintensity localizations on the side of the surgery essentially overlap, PC-T2FLAIR hyperintensities most consistently recapitulate T2W signal. In contrast, abrogation of subarachnoid fluid suppression is minimal in the contralateral frontal cortex.

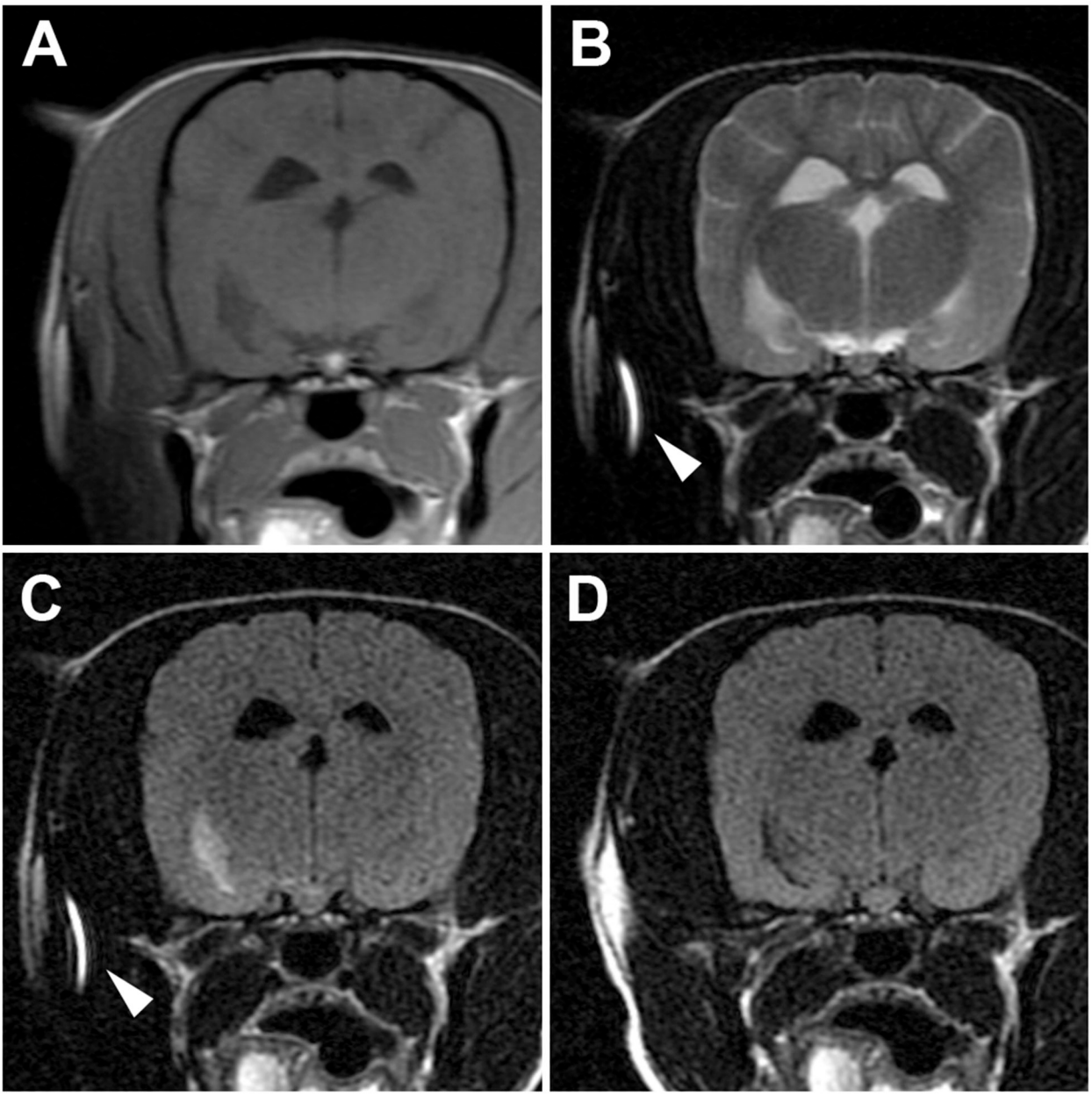

Fig 8.

T1W (A), T2W (B), FLAIR (C, D) images all acquired pre-contrast administration. Regional loss of suppression of CSF signal from the temporal horn of the lateral ventricle (C) has occurred secondary to local field inhomogeneity due to the presence of a metallic endotracheal cuff spring (arrow heads). Suppression is reestablished following removal of the metallic spring (D).

Table 1

Clinical Patient MRI Sequence Parameters

Sequence parameter	T1W	T2W	T2 FLAIR
Repetition time (ms)	516.6–1050	5000	8002
Echo time (ms)	8.9–16.92	97.7–104.6	120.9–125.82
Inversion time (ms)	-	-	2000
Number of excitations	4	3	2
Echo train length	3	23	1

Table 2

Factors and Levels Tested During *in vitro* Evaluation of Tissue Composition and Gadopentetate Concentration on Signal Intensity

Factor	Levels
Tissue	Ultrapure water Water + 2.4g/dL albumin 2% w/v agarose
Gadopentetate concentration (mM)	0, 0.008, 0.023, 0.069, 0.139, 0.278. 0.556, 1.11, 2.22, 6.67, 20.0

Table 3

Pulse Sequence Parameters for *in vitro* MRI Experiments

Sequence parameter	T1W	T2W	FLAIR
Repetition time (ms)	400	4000	8002
Echo time (ms)	11.5	126.9	123.8
Inversion time (ms)	-	-	1800
Number of excitations	4	4	1
Echo train length	3	23	1